Measurements of $2s\ ^2S_{1/2}-2p\ ^2P_{3/2,1/2}$ transition energies in lithiumlike heavy ions: Experiments and results for Ni^{25+} and Zn^{27+}

U. Staude, Ph. Bosselmann, R. Büttner, D. Horn, and K.-H. Schartner
I. Physikalisches Institut der Justus-Liebig-Universität, D-35392 Giessen, Germany

F. Folkmann
Institute of Physics and Astronomy, University of Aarhus, DK-8000 Aarhus, Denmark

A. E. Livingston
Department of Physics, University of Notre Dame, Notre Dame, Indiana 46556

T. Ludziejewski and P. H. Mokler
Gesellschaft für Schwerionenforschung Darmstadt mbH, D-64291 Darmstadt, Germany

(Received 7 May 1998)

Wavelengths of the fine-structure transitions $2s\ ^2S_{1/2}-2p\ ^2P_{3/2}$ and $2s\ ^2S_{1/2}-2p\ ^2P_{1/2}$ in lithiumlike Ni^{25+} and Zn^{27+} have been measured using beam-foil excitation and grazing-incidence spectroscopy. The respective transition wavelengths of 142.461 ± 0.006 Å and of 216.061 ± 0.011 Å for Zn^{27+} have not been measured so far and present the most precise values in lithiumlike heavy ions measured by beam-foil spectroscopy. The Ni^{25+} results are in very good agreement with data from grazing-incidence spectroscopy at tokamaks. The measurement precision for both ions corresponds to less than or equal to 1% of the quantum electrodynamic contributions to the transition energies. This provides sensitivity to two-photon exchange processes for the screening of the electron self-energy. [S1050-2947(98)04310-8]

PACS number(s): 31.30.Jv, 32.30.Jc, 34.50.Fa, 29.40.Gx

I. INTRODUCTION

Precise experimental $2s$-$2p$ transition energies of heliumlike and lithiumlike heavy ions are needed for testing the theory of atomic structure, including electron correlations, as well as relativistic and quantum electrodynamic (QED) contributions. Due to the strong Z dependence of the latter two contributions, the intermediate- and high-Z range is of special interest. In recent years much progress has been made in the *ab initio* calculation of the transition energy in few-electron ions [1–9]. Different achievements are, e.g., the calculations of two-photon exchange processes in describing the screening effects [8] and the calculation of higher-order terms of the Breit interaction [9].

For lithiumlike ions the most successful methods to calculate the $2s$-$2p$ transition energies are at present the multiconfiguration Dirac-Fock method applied by Kim *et al.* [6], the relativistic many-body perturbation theory technique applied by Johnson *et al.* [7] and Blundell [8], and a large-scale relativistic configuration-interaction calculation presented by Chen *et al.* [9]. The earlier calculation of Kim *et al.* [6] used the ''ρ method'' to calculate the QED contribution to the transition energy. This is a phenomenological approximation based on accurately known hydrogenic values. Blundell [8] and Chen *et al.* [9] evaluated the QED corrections using a rigorous formalism based on realistic atomic potentials including screening and screening correction effects [8] of the Lamb shift, which reduces the self-energy contribution. These are the effects that one would like to test systematically in precise measurements along the isoelectronic series in the intermediate- and high-Z range.

In the lithiumlike isoelectronic sequence for heavy ions such accurate experiments have been performed by observation of solar flares ($Z\leqslant26$) [10–12], by using plasma spectroscopy at tokamaks [13–17] ($Z\leqslant36$, $Z=42$), by spectroscopy at an electron-beam ion trap (EBIT) [18–20] ($Z=83,90,92$, 1/2-3/2 transition), by accelerator-based beam-foil spectroscopy [21] ($Z=36$), and by Doppler tuned spectroscopy [22] ($Z=92$, 1/2-1/2 transition only). The measurements have demonstrated that with the relative precisions less than or equal to 2×10^{-4} of the $2s$-$2p$ transition energy, the QED contributions for the heaviest ions can be tested to within a few times 10^{-3}, which corresponds to a sensitivity for the Lamb shift screening at the 1% level.

In the heliumlike isoelectronic sequence $2s$-$2p$ transitions have not been reported for $Z>10$ at tokamaks and EBITs. A recent precision beam-foil wavelength measurement for the $1s2s\ ^3S_1-1s2p\ ^3P_{0,2}$ fine-structure transitions in heliumlike Ar^{16+} ions [23] suggested that the calculated QED contribution to the $1s2s\ ^3S_1$ state energy should be reduced by about 1%, corresponding to $0.15(Z\alpha)^4$ a.u.

For few-electron ions, due to the larger relative QED contribution to the transition energy, the $2s$-$2p$ measurements provide higher-precision QED tests than $1s$-$2p$ measurements [24]. In the hydrogen isoelectronic sequence, $1s$-$2p$ measurements are sensitive to the $1s$ Lamb shift in heavy systems such as gold and uranium at the 3% level [25,26], whereas $2s$-$2p$ measurements achieve an order of magnitude better QED test of 0.2% [22].

In the present work we report wavelength measurements of the $2s\ ^2S_{1/2}-2p\ ^2P_{3/2,1/2}$ transitions in lithiumlike Ni^{25+} and Zn^{27+} ions with precisions less than 1×10^{-4}. In the case of Ni our result provides a precise beam-foil value for

comparison with data from tokamak sources [13,15] and it allows a critical test of our experimental installation for future experiments with heavier heliumlike and lithiumlike ions. The $2s$-$2p$ transition wavelengths for the heavier Zn ion have not been measured so far.

The experiment and the wavelength-scale calibration procedure are discussed in detail. A comparison with the previous measurements in lithiumlike Ni at tokamaks and with the above-mentioned calculations is carried out. In another paper [27] we plan to present further results of an experiment with Ag^{44+} in connection with a summary of experiments along the isoelectronic sequence of lithiumlike ions.

II. EXPERIMENT

A. General description

The Ni and Zn experiments were performed at the heavy-ion accelerator UNILAC of the GSI using 5.888-MeV/nucleon and 11.52-MeV/nucleon Ni^{9+} ions and 5.894-MeV/nucleon Zn^{10+} ions. The ions were excited in 200-μg/cm^2 carbon foils. Under these conditions berylliumlike and lithiumlike ions at the lower projectile energy and lithiumlike and heliumlike ions at the higher energy are most strongly produced by the ion-foil interaction [28]. The light emitted from the foil excited ions was observed with the GSI 5-m grazing-incidence vacuum ultraviolet (vuv) spectrometer [29] as described in Sec. II B (see also Fig. 1). The optical axis was oriented 90° with respect to the ion-beam direction. The measured wavelengths require a Doppler shift correction. The spectrometer is equipped with a 270-lines/mm spherical grating and a two-dimensional position-sensitive microchannel plate (MCP) detector positioned nearly tangential to the Rowland circle. A static *in situ* spectrometer wavelength-scale calibration is used. The observable length of the ion beam is about 200 μm. For the lower energy this corresponds to about a 6-ps time of flight of the ions. The foil displacement with respect to the optical axis of the spectrometer was determined by an optical position encoder fixed to the foil target wheel support and was typically 400 μm. This displacement is not crucial because the shortest lifetime observed in these experiments (Zn^{27+} $2p\ ^2P_{3/2}$) is 129 ps [30,31]. This lifetime corresponds to a decay length of about 4 mm for the lower projectile energy. In most of the measurements we used an entrance slit width of 30 μm and kept the detector and foil position constant. The particle flux was on the order of about 10^{11} particles per second. The ion-beam spot was focused on the target using a thin fluorescent screen consisting of ceramic material instead of the carbon foil. When focused, the ion beam passed through a 3-mm-wide central hole in this screen. The ion current was measured for normalization in a distant well-shielded Faraday cup.

On the average up to 1 h was spent for recording one projectile and calibration spectrum. Except for the 1/2-1/2 transitions in Ni, for each transition about 40–60 spectra were taken. The 1/2-1/2 transition in Ni was measured five times with the lower energy, 2–3 h each. In addition, two spectra were taken at the higher energy, for 2.5 h with a 30-μm entrance slit and for 5.5 h with a 50-μm entrance slit.

Normally, after measuring several spectra under identical conditions, some experimental parameters were changed. By

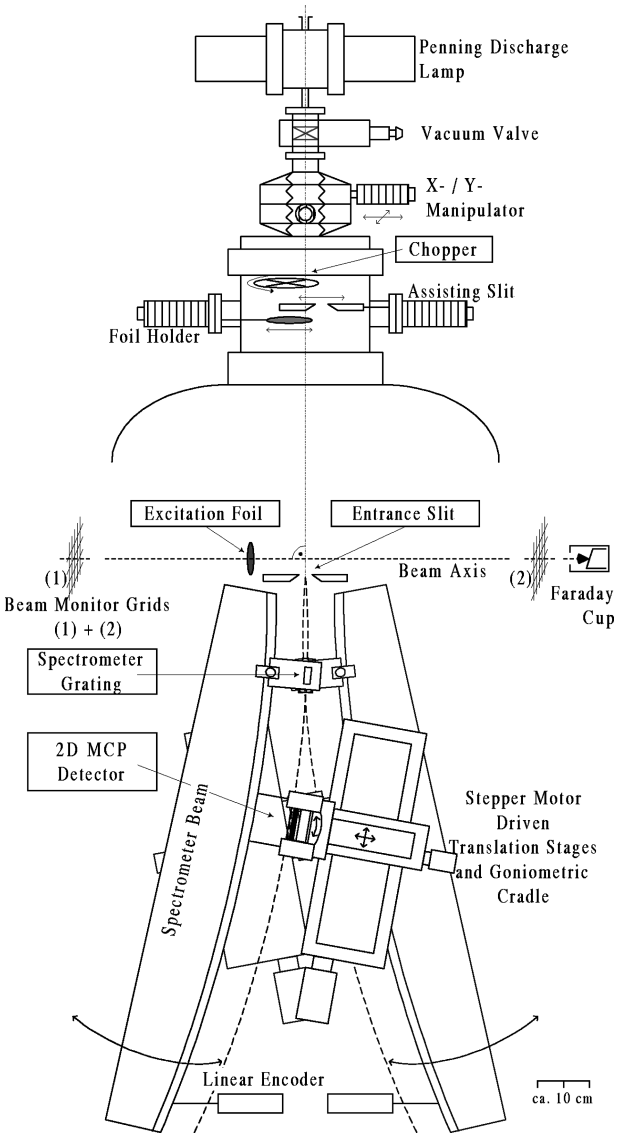

FIG. 1. Beam-foil spectroscopy setup of the GSI 5-m grazing-incidence spectrometer equipped with a Penning discharge lamp for a static wavelength-scale calibration. 2D MCP denotes two-dimensional microchannel plate.

that we ensured that such actions did not effect the measured wavelength. As an example the detector was moved along the Rowland circle to bring the same spectra to different detector positions, which is important in the case of local nonlinearities of the detector system. Also the position of the calibration light source was shifted perpendicular to the beam axis to check for an influence of different illuminations of the grating and the detector. The target foil position was changed to exclude a shadowing of the target wheel. The most important variation was the turning of the spectrometer by 180° around the optical axis. This special feature of the GSI 5-m grazing-incidence vuv spectrometer (as described in Sec. II B) has not been used so far in our experiments. Turning the spectrometer in this way means that a selected point on the grating views the ion beam at a different angle while the mean angle of observation remains the same. This option is of special interest for Doppler broadened line shapes in combination with the static wavelength-scale calibration. If an area of the grating is illuminated by Doppler redshifted

light in one case, in the other case the same area will be illuminated by blueshifted light. If the response of the grating varies locally a shift of the determined wavelength may be expected. Averaging the two results allows a partial suppression of grating response asymmetry.

The production of calibration lines for establishing the spectrometer wavelength scale is not an easy task, especially in the (100–200)-Å range. Our earlier experiments with xenon and krypton [32,33] used an in-beam calibration based on calculated energies of Rydberg transitions in hydrogenlike and heliumlike ions. The latter depend on the population of the l levels, which is not accurately known. As a consequence, modeling of the l distributions is necessary and results in calibration lines that are approximately one order of magnitude less accurately known than some reference lines from light elements [13]. On the other hand, this procedure avoids the need for a correction of the Doppler shift.

In the present experiments a powerful Penning discharge lamp [34] was installed for a static *in situ* spectrometer wavelength-scale calibration. The calibration spectrum from the Penning discharge lamp is registered simultaneously and continuously with the projectile spectrum, a procedure necessary to minimize the influence of drifts in the detector system. For this purpose a chopper wheel synchronized with the UNILAC macropulse was installed between the Penning discharge lamp and the entrance slit of the spectrometer. In combination with our position-analysis program [35], the simultaneous accumulation of two different spectra is possible, using the 50-Hz macropulse with (2–4)-ms pulse time as a gating signal. In addition to the online evaluation, each individual event, including the corresponding gate signal, is stored in a listmode file. Thus, after the beam time a reevaluation can be performed to achieve optimized spectra, for example, with regard to a better signal-to-noise ratio and improved resolution. Examples of simultaneous projectile and calibration spectra are given in Figs. 2 and 3. The Penning discharge lamp could be operated continuously for about 6 h. Then, due to sputter erosion, the Al cathodes had to be replaced.

B. Apparatus

The GSI 5-m grazing-incidence vuv spectrometer is schematically shown in Fig. 1. It is mounted in a cylindrical vacuum vessel approximately 1.8 m in height and 1 m in diameter. A mechanical support (''spectrometer beam'') of high precision and stability serves as a reference for the Rowland circle (5 m in diameter). The 270-lines/mm spectrometer grating, blazed at an angle of 2°, is fixed on this spectrometer beam, which may be pivoted about the spectrometer entrance slit in order to vary the angle of observation. The detector, which consists of a 40-mm-wide microchannel plate chevron cascade pair followed by a wedge-and-strip anode for position readout, is moved by two stepper motor driven linear stages and one stepper motor driven goniometric cradle. The adjustment of the detector in relation to the Rowland circle is performed using two optical position encoders to determine the distance and angle between the detector surface and the spectrometer beam. For data accumulation standard nuclear instruments module electronic and customized interface hardware and software [35–37] are used.

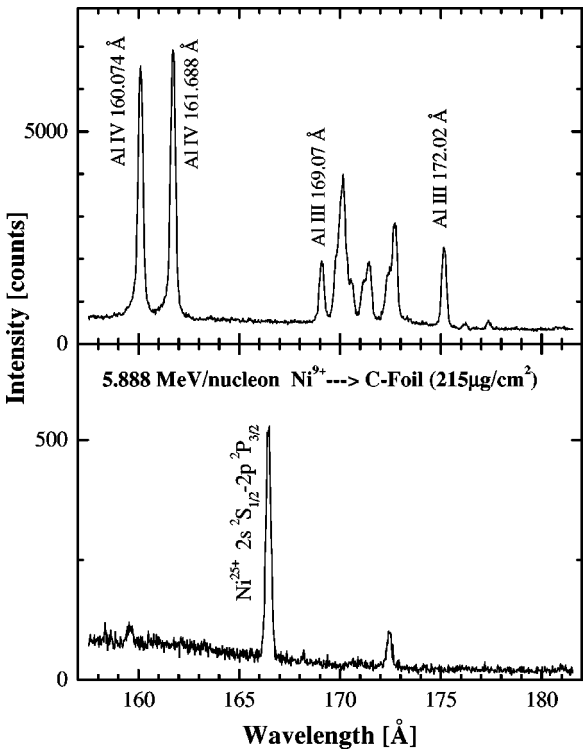

FIG. 2. The $2s\ ^2S_{1/2}-2p\ ^2P_{3/2}$ line of lithiumlike Ni^{25+} and Al IV and Al III calibration lines registered simultaneously and continuously using a chopper wheel synchronized with the UNILAC macropulse (with a measurement time of approximately 4 h).

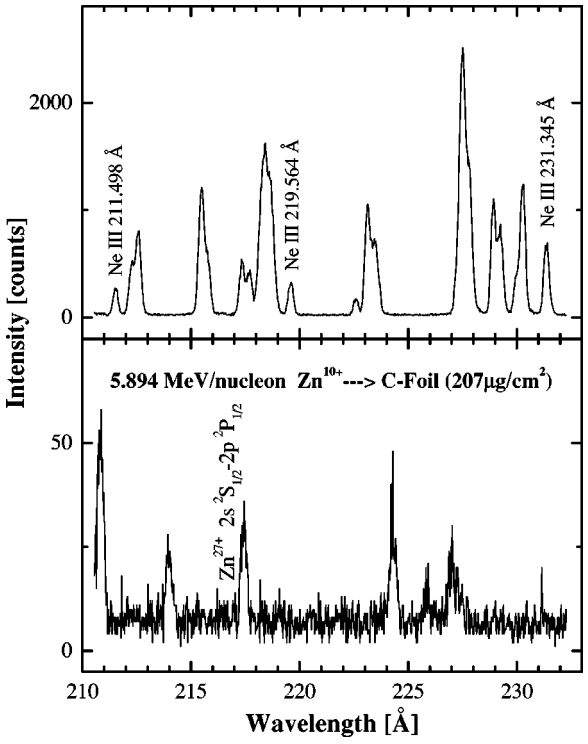

FIG. 3. The $2s\ ^2S_{1/2}-2p\ ^2P_{1/2}$ line of lithiumlike Zn^{27+} (and in addition some lines in Zn^{26+}) and Ne III calibration lines registered simultaneously and continuously (with a measurement time of approximately 1 h).

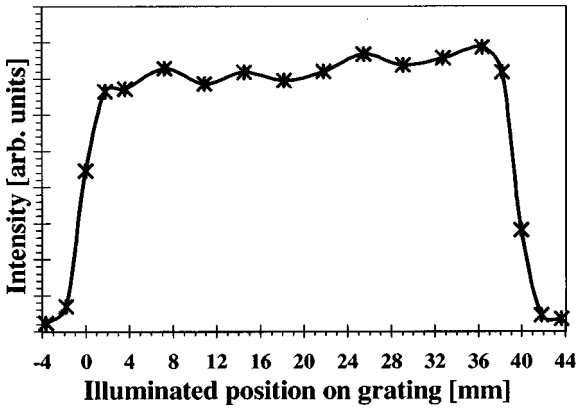

FIG. 4. Normalized reflected intensity as a function of the selected illuminated portion of the grating for an Al IV calibration line at 160.074 Å.

A special feature of the spectrometer is the possibility of turning the complete spectrometer (i.e., the entrance slit, the grating, and the detector) by 180° around the optical axis without breaking the vacuum. This advantage of an online first-order correction for an observation angle misalignment has been mentioned in Sec. II A.

The Penning discharge lamp is mounted on the top of a small vacuum chamber, which itself is connected to the hemispherical spectrometer dome. The alignment of the Penning discharge lamp to the optical axis of the spectrometer is performed with an X-Y manipulator. For maintenance the Penning discharge lamp may be removed without breaking the vessel vacuum.

Below the Penning discharge lamp a chopper wheel enables the synchronization of the calibration spectrum and the projectile spectrum from the pulsed ion beam by periodic shadowing of the light emitted from the calibration source. In addition, a 100-μm-wide assisting slit and a foil holder are each mounted on a linear micrometer feedthrough. The slit is used in the setup procedure for the alignment of the angle of observation to 90° [38]. Using the assisting slit and the entrance slit, a narrow photon beam from the Penning discharge lamp can be formed. By pivoting the spectrometer beam about the entrance slit, the grating response as a function of the illuminated portion can be studied for selected dispersed wavelengths. The result of such a measurement is given in Fig. 4 for $\lambda = 160.074$ Å, an Al IV line used for calibration in the Ni experiment. Only a slight linear variation of the local response was observed. A measurement at $\lambda = 227.5$ Å (a Ne III calibration line) gave the same result. Figure 4 demonstrates the quality of the grating, which is a master grating ruled by Hyperfine Inc., Boulder, Colorado on a 40-mm-wide area of a 50×50 mm^2 gold coated blank. We conclude that the wavelength calibration is not disturbed by grating asymmetries. As a consequence, no systematic difference between wavelengths from the two spectrometer positions was observed.

The foil holder enables the reduction of the light intensity of the Penning discharge lamp, e.g., by use of a 100-μg/cm^2 aluminum foil, to match the intensities of the projectile spectrum and the calibration spectrum. The foil holder and slit may be moved out of the optical axis if not used. Along the ion-beam axis two beam monitor grids (separated by 3.4 m) are located in front of and behind the spectrometer to determine the inclination of the ion-beam axis with respect to its default axis. The beam line is terminated in a shielded Faraday cup.

C. Measurement procedure

1. Position linearity of the detector

As mentioned in Sec. II B, a position-sensitive detector based on a wedge-and-strip readout was used. To adjust its electronic components, in a first step, test pulses of various heights were sent through a capacitor into each of the preamplifiers; the output numbers of the three analog-to-digital converter (ADC) units were recorded, while the amplification and the ADC zero levels were varied. This procedure was repeated until the same total amplification and zero offset for all three channels of the position read out was obtained, including cross talk contributions. In a second step, the outcome of the electronic adjustment was tested using a mask with 20 slits 75 μm wide and 44 mm long, which was fixed on the detector. The accuracy of the slit position is 5 μm. In the case of Ni, in addition, a 70-μm-wide slit, illuminated with light of a helium discharge, was moved in steps of 0.5 mm across the detector. Test spectra were recorded and the line positions were fitted. A linear least-squares fit through the data points shows characteristic and reproducible deviations from linearity. For the detector used in the Ni experiment they correspond to an integral nonlinearity of 2×10^{-3}, while for the Zn experiment with a different wedge-and-strip anode 5×10^{-4} was measured. In the detector tests, as well as in the beam-foil experiments, the single events were stored in listmode, enabling a correction procedure for minimizing the residual nonlinearity. A software routine allowed a reduction of the final nonlinearity to 5×10^{-4} in the case of Ni and 3×10^{-4} in the case of Zn. The corresponding error appears in the uncertainty of the wavelength result.

2. Wavelength scale

The dispersion of the spectrometer along the flat channel plate detector has been studied extensively. An analytical description, taking into account the angle between the detector surface and the tangent to the Rowland circle, yields a complex formula. Investigations of this formula showed that the dispersion on the detector is quadratic for the detector parameters used in our experiments, with a negligible error. Thereby the static *in situ* spectrometer wavelength-scale calibration was established by use of three or four well known calibration lines emitted by the Penning discharge lamp. Depending on the wavelength region, spectral lines emitted from aluminum (sputtered cathode material inside the Penning discharge lamp) or helium and neon (gas fed into the Penning discharge lamp) were used. The lines were produced in a gas discharge of typically 600 V and 500 mA. The calibration spectra were measured simultaneously with those of the projectiles. The separation of the two kinds of spectra was performed by use of the 50-Hz macrostructure of the ion beam and the synchronized chopper wheel. Examples are shown in Figs. 2 and 3.

In the case of the Ni 1/2-3/2 transition (Fig. 2), isolated aluminum lines were used. The wavelengths of the two strong unblended Al IV lines at 160.074 Å and 161.688 Å are

TABLE I. Summary of individual contributions to the experimental uncertainty of the $2s\ ^2S_{1/2}-2p\ ^2P_{1/2}$ wavelength in lithiumlike Ni^{25+}.

	Contribution	
Error source	(mrad)	(mÅ)
statistical		5
local detector nonlinearity		13
uncertainty of calibration line wavelengths		4
total for Doppler shifted wavelength		14
adjustment of the angle of observation	0.28	7
reproducibility of the angle of observation	0.10	3
determination and stability of the center of the ion beam	0.13	3
ion-beam velocity behind the excitation foil		4
total for Doppler correction		9
Total		17

known to within 0.004 Å and are suitable as wavelength references [39]. The wavelengths of the Al III lines at 169.07 Å and 175.02 Å were determined by Finkenthal *et al.* [40] with an accuracy of 0.01 Å. Thus the Al III lines are less suitable as reference lines, but at least one of them, preferable the unblended line at 169.07 Å, must be used for a determination of the quadratic spectrometer dispersion.

In the case of the Ni 1/2-1/2 transition, unblended Ne III lines at 231.345 Å, 238.194 Å, and 240.937 Å were used with an accuracy of 0.001 Å. The identifications are based on the work of Livingston *et al.* [41], while the predicted wavelengths are based on the precisely established energy levels described by Persson *et al.* [42]. Furthermore, one Ne IV line at 234.316 Å [43] was taken into account.

In the case of the Zn 1/2-3/2 transition (measured in second order of diffraction), unblended Ne III lines at 282.497 Å, 301.125 Å, 308.568 Å, and 313.058 Å [44] were used. In addition, one transition in He II at 303.782 Å [44] was used.

In the case of the Zn 1/2-1/2 transition (Fig. 3), unblended Ne III lines at 211.498 Å, 219.564 Å, and 231.345 Å, with an accuracy of 0.001 Å, were used [41]. The other Ne III lines in Fig. 3 have a multiplet structure that was resolved for a slit width of 5 μm.

3. Doppler shift correction

The ion-beam velocity amounts to more than 10% of the speed of light. Thus a correction of the Doppler shift is necessary and accordingly the ion-beam velocity and the angle of observation had to be measured. The Doppler shifted wavelength λ' and the wavelength λ_0 in the projectile system are related according to $\lambda' = \lambda_0 \gamma(1-\beta \cos\theta)$, where β is the ion-beam velocity in units of the speed of light, γ is the relativistic time dilation factor, and θ is the angle of observation.

The ion-beam velocity is measured by a time-of-flight method as a standard procedure for the accelerator [45]. The energy loss of the ions inside the target foil was estimated by use of the work of Hubert *et al.* [46] and calculations with the GSI ATIMA code based on [47]. Pivoting the spectrometer beam about the entrance slit, the angle of observation is precisely set to 90° with relation to the default beam axis by an iterative procedure using an optical beam-splitter cube, an autocollimation telescope, a measuring telescope, and the assisting slit in the upper part of the spectrometer. A calibrated telescope support serves as a reference for the default beam axis. This setup procedure is performed independently for the two possible positions of the spectrometer separated by 180°. The position of the ion beam on the beam monitor grids was measured frequently and deviations were used in the Doppler shift correction. An example of the good stability of the beam center is a mean deviation of ± 1100 μm of the centers of gravity of the beam profile with respect to its mean value for a 55-h period of the Ni beam time at low energy. This corresponds to an uncertainty of the angle of observation of 1.7 mrad. Even at an observation angle of 90° the transverse component of the Doppler shift is observed. Due to the high velocity, the Doppler shift of the wavelengths is of the order of 1%.

4. Error discussion

A careful analysis of the contributing errors has been carried out. The individual contributions are given in Table I for the case of the 1/2-1/2 transition in Ni as an example. This is representative of the other results presented, except that in the case of Zn the uncertainty due to the local detector nonlinearity has been reduced to 6 mÅ by use of the new detector. The data represent weighted mean values of repeated measurements of beam-foil and calibration spectra. All independent uncertainties were added quadratically.

The uncertainties may be divided into two parts. One part belongs to the determination of the Doppler shifted wavelength. It includes the statistical uncertainties of the beam and the calibration lines, the uncertainty due to the local nonlinearity of the detector, and the uncertainty of the wavelengths of the calibration lines. The contributions of the calibration lines are determined in the following way. Each calibration line was varied over the range of its uncertainty (e.g., ± 1 mÅ for the uncertainty of the wavelength of a Ne III line). An iterative procedure for all used calibration lines, taking the two extreme and the mean value of the calibration wavelengths, yields slightly different Doppler shifted projectile wavelengths for each selected spectrum (for example, 27 values for use of three calibration lines or 81 values for use of four calibration lines). The standard deviation of these

values is treated as the resulting uncertainty for the projectile wavelength.

The second part is connected to the Doppler shift correction. Here the uncertainties of the angle of observation and the velocity of the ions have to be taken into account. The procedure of setting the angle of observation to 90° before the measurements, the agreement with the verification after the measurements (stability of the angle of observation), the determination and the stability of the center of the ion beam on the beam monitor grids, and the uncertainty in the position of the beam monitor grids contribute to the uncertainty of the observation angle. The leading uncertainty of the ion-beam velocity results from the energy loss in the excitation foil. Here the foil thickness uncertainty contributes at the same order of magnitude as the energy loss itself. The Doppler shift correction produces errors according to $\Delta\lambda_0/\lambda_0 \approx \Delta\theta\beta+\Delta\beta/\beta\beta^2$, with $\Delta\theta$ denoting the uncertainty of the angle of observation and $\Delta\beta/\beta$ the relative uncertainty of the ion-beam velocity. Fortunately, the influence from the relative uncertainty of the ion-beam velocity is reduced by the factor β^2, which amounts to two orders of magnitude for the relevant ion-beam velocities of $\beta\approx 0.1$. Also the uncertainty of the angle of observation is reduced by one order of magnitude going to the relative wavelength uncertainty.

III. RESULTS

The wavelength of the $2s\ ^2S_{1/2}-2p\ ^2P_{3/2}$ transition in lithiumlike Ni was determined to be 165.406 ± 0.015 Å, corresponding to 604 573(56) cm^{-1} or 74.958(7) eV. The relative uncertainty of this result is 9×10^{-5}. The wavelength of the $2s\ ^2S_{1/2}-2p\ ^2P_{1/2}$ transition in lithiumlike Ni was determined to be 234.168 ± 0.017 Å, corresponding to 427 044(32) cm^{-1} or 52.947(4) eV from the measurements with lower energy. The relative uncertainty of this result is 7×10^{-5}. Two measurements with the higher energy, which were intended to observe a transition in heliumlike Ni, yield 234.162 ± 0.034 Å and 234.191 ± 0.040 Å and are in good agreement with the low-energy value presented here.

The wavelength of the $2s\ ^2S_{1/2}-2p\ ^2P_{3/2}$ transition in lithiumlike Zn was determined to be 142.461 ± 0.006 Å, corresponding to 701 946(30)cm^{-1} or 87.030(4) eV. The relative uncertainty of this result is 4×10^{-5}. The wavelength of the $2s\ ^2S_{1/2}-2p\ ^2P_{1/2}$ transition in lithiumlike Zn was determined to be 216.061 ± 0.011 Å, corresponding to 462 832(24) cm^{-1} or 57.384(3) eV. The relative uncertainty of this result is 5×10^{-5}.

IV. DISCUSSION

We compare our Ni^{25+} result with previous measurements and with calculations in Figs. 5 and 6. The wavelengths of the 1/2-3/2 and 1/2-1/2 transitions were measured rather precisely at tokamaks by Hinnov and Denne [13] and Sugar *et al.* [15]. The present results show very good agreement with these earlier measurements. Also beam-foil measurements are available for comparison, in the case of the 1/2-3/2 transition by Büttner *et al.* [38] and in the case of the 1/2-1/2 transition by Zacarias *et al.* [48]. A comparison of all data is given in Table II. The comparison with the older beam-foil result of Büttner *et al.* [38] manifests the present improvement of our technique. A general maintenance of the spectrometer, a new spectrometer grating, a new detector, and the herein introduced technique of turning the spectrometer by 180° about the observation axis yield increased accuracy. Also moving the spectrometer to another accelerator beam line was advantageous for reduction of the background. The tokamak measurements have slightly smaller error bars due to the negligible Doppler shift correction and to more accurately known calibration lines, emitted *in situ* with the studied line. Nevertheless, the present results are of comparable accuracy. This is important especially in view of scheduled measurements at higher Z, where the beam-foil method is more favorable. It is emphasized that an apparent systematic difference between wavelengths observed at tokamaks and those using the beam-foil technique [21,49] is not confirmed by the presented measurements. The QED contribution to the transition energies in Ni is 0.8% (1/2-3/2) and 1.2% (1/2-1/2) [9]. Thus the presented results for Ni are sensitive to 1% and 0.6% of the QED contribution, respectively.

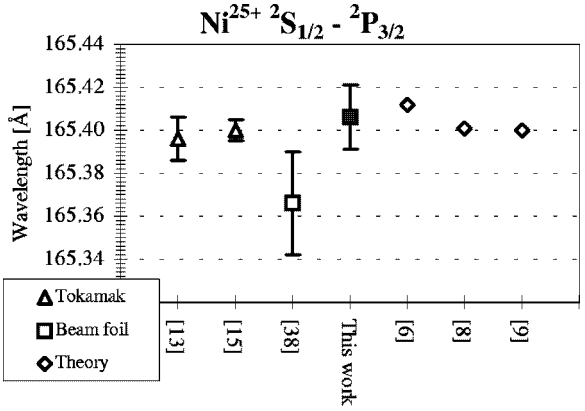

FIG. 5. Comparison of our wavelength result for the $2s\ ^2S_{1/2}-2p\ ^2P_{3/2}$ transition in Ni^{25+} with previous measurements (by Hinnov and Denne [13], Sugar *et al.* [15], and Büttner *et al.* [38]) and calculations (by Kim *et al.* [6], Blundell [8], and Chen *et al.* [9]).

For Zn the relative uncertainty is smaller than in the case of Ni. The major reason is an improvement in the detector

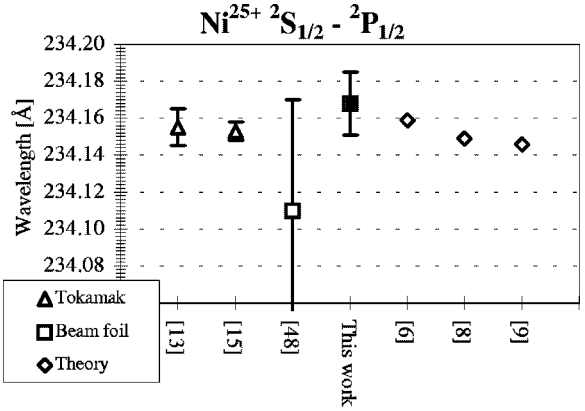

FIG. 6. Comparison of our wavelength result for the $^2S_{1/2}-2p\ ^2P_{1/2}$ transition in Ni^{25+} with previous measurements (by Hinnov and Denne [13], Sugar *et al.* [15], and Zacarias *et al.* [48]) and calculations (by Kim *et al.* [6], Blundell [8], and Chen *et al.* [9]).

TABLE II. Experimental results for the wavelengths of the $2s\ ^2S_{1/2}-2p\ ^2P_{3/2,1/2}$ transitions in lithium-like Ni^{25+} and Zn^{27+} ions (in angstroms) compared with previous experimental results and with calculations.

Results	Ni 1/2–3/2	Ni 1/2–1/2	Zn 1/2–3/2	Zn 1/2–1/2
Experimental				
this work	165.406(15)	234.168(17)	142.461(6)	216.061(11)
Hinnov and Denne [13]	165.396(10)	234.155(10)		
Sugar *et al.* [15]	165.400(5)	234.153(5)		
Zacarias *et al.* [48]		234.110(60)		
Büttner *et al.* [38]	165.366(24)			
Theory				
Kim *et al.* [6]	165.412	234.159	142.474	216.072
Blundell [8]	165.401	234.149	142.457	216.042
Chen *et al.* [9]	165.400	234.146	142.459	216.059

system. The QED contribution to the transition energies in Zn is 0.9% (1/2-3/2) and 1.4% (1/2-1/2) [9]. Thus the present results for Zn are sensitive to 0.5% and 0.4% of the QED contribution, respectively.

V. COMPARISON WITH CALCULATIONS

Figures 5 and 6 and Table II show also the calculations of Kim *et al.* [6], Blundell [8], and Chen *et al.* [9]. We obtained interpolated results for $Z=28$ from Blundell [50] and we performed a cubic spline interpolation for the values of Chen *et al.* [9] for $Z=28$ and 30. As was outlined briefly in the Introduction, the calculations are based on different methods and evaluate different higher-order contributions. Among the error bars there is very good agreement between experiments and all three calculations. Within the calculations, Blundell [8] and Chen *et al.* [9] agree much better with each other than with Kim *et al.* [6]. Nevertheless, when comparing the single non-QED and QED contributions, Blundell [8] and Chen *et al.* [9] differ more than they do in the total transition energy. As mentioned by Chen *et al.* [9], there are partial cancellations of different contributions to the total transition energy in these calculations. It is evident that at present experiments cannot distinguish between these calculations and additional data along the isoelectronic sequence are needed. An extension of the measurements to higher-Z values is planned to be reported elsewhere [27].

VI. CONCLUSIONS

The present measurements belong to a series of experiments that test the structure of heavy few-electron ions and hence the theoretical achievements in the calculation of the transition energies. Our results for the lithiumlike $2s$-$2p$ transition energies for $Z=28$ and $Z=30$ provide relative uncertainties as low as 4×10^{-5}. With this precision, measurements become sensitive to the smallest QED contributions considered so far in the calculations for lithiumlike ions. We obtained very good agreement with results from spectroscopy at tokamaks. This demonstrates that beam-foil spectroscopy is appropriate for measurements up to the largest Z values for the $2s$-$2p$ transitions, which are not accessible at tokamaks. These future measurements will profit from the increase of the relative QED contributions with increasing values of Z. Still, efforts should be undertaken to reduce the experimental errors. This should be possible with detectors of extreme linearity and with even more refined optical alignment procedures.

ACKNOWLEDGMENTS

We gratefully acknowledge the skillful help of Dr. J. Klabunde and L. Dahl as well as the operators running the UNILAC. We emphasize the enthusiastic technical assistance of A. Bardonner (GSI). We thank Dr. R. Speer, Imperial College London, for assistance in mounting the new grating. A.E.L. acknowledges partial support from the U.S. Department of Energy, Division of Chemical Sciences. The experiment is supported by the German Minister for Research and Technology under Contract No. 06 GI 846, by the GSI collaborative research program, and by a NATO travel grant.

[1] I. Lindgren, H. Persson, S. Salomonson, and P. Sunnergren, Phys. Scr. **T59**, 179 (1995).

[2] K. T. Cheng, W. R. Johnson, and J. Sapirstein, Phys. Rev. Lett. **66**, 2960 (1991).

[3] D. R. Plante, W. R. Johnson, and J. Sapirstein, Phys. Rev. A **49**, 3519 (1994).

[4] I. Lindgren, H. Persson, S. Salomonson, and L. Labzowsky, Phys. Rev. A **51**, 1167 (1995).

[5] E. Lindroth, Nucl. Instrum. Methods Phys. Res. B **98**, 1 (1995).

[6] Y.-K. Kim, D. H. Baik, P. Indelicato, and J. P. Desclaux, Phys. Rev. A **44**, 148 (1991).

[7] W. R. Johnson, S. A. Blundell, and J. Sapirstein, Phys. Rev. A **37**, 2764 (1988).
[8] S. A. Blundell, Phys. Rev. A **47**, 1790 (1993).
[9] M. H. Chen, K. T. Cheng, W. R. Johnson, and J. Sapirstein, Phys. Rev. A **52**, 266 (1995).
[10] K. P. Dere, Astrophys. J. **221**, 1062 (1978).
[11] G. D. Sandlin, G. E. Brueckner, V. E. Scherrer, and R. Tousey, Astrophys. J. **205**, L47 (1976).
[12] K. G. Widing, and J. D. Purcell, Astrophys. J. **204**, L151 (1976).
[13] E. Hinnov and B. Denne, Phys. Rev. A **40**, 4357 (1989).
[14] R. J. Knize, Phys. Rev. A **43**, 1637 (1991).
[15] J. Sugar, V. Kaufman, and W. L. Rowan, J. Opt. Soc. Am. B **9**, 344 (1992).
[16] J. Sugar, V. Kaufman, and W. L. Rowan, J. Opt. Soc. Am. B **10**, 13 (1993).
[17] J. Reader, J. Sugar, N. Acquista, and R. Bahr, J. Opt. Soc. Am. B **11**, 1930 (1994).
[18] P. Beiersdorfer, D. Knapp, R. E. Marrs, S. R. Elliott, and M. H. Chen, Phys. Rev. Lett. **71**, 3939 (1993).
[19] P. Beiersdorfer, A. Osterheld, S. R. Elliott, M. H. Chen, D. Knapp, and K. Reed, Phys. Rev. A **52**, 2693 (1995).
[20] P. Beiersdorfer, A. Osterheld, J. Scofield, J. Crespo López-Urrutia, and K. Widmann, Phys. Rev. Lett. **80**, 3022 (1998).
[21] S. Martin, A. Denis, M. C. Buchet-Poulizac, J. P. Buchet, and J. Désesquelles, Phys. Rev. A **42**, 6570 (1990).
[22] J. Schweppe, A. Belkacem, L. Blumenfeld, N. Claytor, B. Feinberg, H. Gould, V. E. Kostroun, L. Levy, S. Misawa, J. R. Mowat, and M. H. Prior, Phys. Rev. Lett. **66**, 1434 (1991).
[23] K. W. Kukla, A. E. Livingston, J. Suleiman, H. G. Berry, R. W. Dunford, D. S. Gemmell, E. P. Kanter, S. Cheng, and L. J. Curtis, Phys. Rev. A **51**, 1905 (1995).
[24] R. E. Marrs, S. R. Elliott, and Th. Stöhlker, Phys. Rev. A **52**, 3577 (1995); Th. Stöhlker and A. E. Livingston, Acta Phys. Pol. B **27**, 441 (1996).
[25] H. F. Beyer, IEEE Trans Instrum. Meas. **44**, 510 (1995); H. F. Beyer, G. Menzel, D. Liesen, A. Gallus, F. Bosch, R. Deslattes, P. Indelicato, Th. Stöhlker, O. Klepper, R. Moshammer, F. Nolden, H. Eickhoff, B. Franzke, and M. Speck, Z. Phys. D **35**, 169 (1995).
[26] Th. Stöhlker, P. H. Mokler, F. Fosch, R. W. Dunford, C. Kozhuharov, G. Menzel, R. Rymuza, Z. Stachura, P. Swiat, A. Warczak, B. Franzke, O. Klepper, A. Krämer, T. Ludziejewski, H. T. Prinz, H. Reich, and M. Steck, GSI Report No. 98-1, 1998.
[27] Ph. Bosselmann, U. Staude, R. Büttner, D. Horn, K.-H. Schartner, F. Folkmann, A. E. Livingston, T. Ludziejewski, and P. H. Mokler (unpublished).
[28] P. H. Mokler, Th. Stöhlker, R. Büttner, and K.-H. Schartner, Nucl. Instrum. Methods Phys. Res. B **83**, 37 (1993).
[29] B. Kraus, K.-H. Schartner, F. Folkmann, A. E. Livingston, and P. H. Mokler, Proc. SPIE **1159**, 217 (1989).
[30] K. T. Cheng, Y.-K. Kim, and J. P. Desclaux, At. Data Nucl. Data Tables **24**, 111 (1979).
[31] C. E. Theodosiou, L. J. Curtis, and M. El-Mekki, Phys. Rev. A **44**, 7144 (1991).
[32] R. Büttner, B. Kraus, K.-H. Schartner, F. Folkmann, P. H. Mokler, and G. Möller, Z. Phys. D **22**, 693 (1992).
[33] R. Büttner, B. Kraus, M. Nicolai, K.-H. Schartner, F. Folkmann, P. H. Mokler, and G. Möller, in *VIth International Conference on the Physics of Highly Charged Ions*, edited by P. Richard, M. Stöckli, C. L. Locke, and C. D. Lin, AIP Conf. Proc. No. 274 (AIP, New York, 1993), p. 423.
[34] D. S. Finley, P. Jelinsky, S. Bowyer, and R. F. Malina, Proc. SPIE **689**, 6 (1986).
[35] U. Staude, diploma thesis, University of Giessen, 1994 (unpublished).
[36] B. Kraus, doctoral thesis, University of Giessen, 1991 [GSI Report No. GSI-91-16 (1991)].
[37] U. Staude, doctoral thesis, University of Giessen, 1998 [GSI Report No. Diss. 98-06 (1998)].
[38] R. Büttner, U. Staude, M. Nicolai, J. Brauckhoff, K.-H. Schartner, F. Folkmann, and P. H. Mokler, Nucl. Instrum. Methods Phys. Res. B **98**, 41 (1995).
[39] V. Kaufman and W. C. Martin, J. Phys. Chem. Ref. Data **20**, 775 (1991).
[40] M. Finkenthal, A. Litman, P. Mandelbaum, D. Stutman, and J. L. Schwob, J. Opt. Soc. Am. B **5**, 1640 (1988).
[41] A. E. Livingston, R. Büttner, A. S. Zacarias, B. Kraus, K.-H. Schartner, F. Folkmann, and P. H. Mokler, J. Opt. Soc. Am. B **14**, 522 (1997).
[42] W. Persson, C.-G. Wahlström, L. Jönsson, and H. O. Di Rocco, Phys. Rev. A **43**, 4791 (1991).
[43] F. W. Paul and H. D. Polster, Phys. Rev. **59**, 424 (1941).
[44] R. L. Kelly, J. Phys. Chem. Ref. Data Suppl. **16** (1), 20 (1987).
[45] P. Strehl, *Handbook of Ion Sources* (CRC, Boca Raton, FL, 1994); H. Geissel, Y. Laichter, R. Albrecht, T. Kitahara, J. Klabunde, P. Strehl, and P. Armbruster, Nucl. Instrum. Methods Phys. Res. B **206**, 609 (1983).
[46] F. Hubert, R. Bimbot, and H. Gauvin, At. Data Nucl. Data Tables **46**, 1 (1990).
[47] T. Schwab, GSI Report No. GSI-91-10, Darmstadt (1991).
[48] A. S. Zacarias, A. E. Livingston, Y. N. Lu, R. F. Ward, H. G. Berry, and R. W. Dunford, Nucl. Instrum. Methods Phys. Res. B **31**, 41 (1988).
[49] B. Denne-Hinnov, Phys. Rev. A **45**, 2135 (1992).
[50] S. A. Blundell (private communication).